

# PEGylated PLGA-based nanoparticles targeting M cells for oral vaccination

Marie Garinot<sup>a</sup>, Virginie Fiévez<sup>a,b</sup>, Vincent Pourcelle<sup>c</sup>, François Stoffelbach<sup>d</sup>, Anne des Rieux<sup>a,b</sup>, Laurence Plapied<sup>a,b</sup>, Ivan Theate<sup>e</sup>, Hélène Freichels<sup>d</sup>, Christine Jérôme<sup>d</sup>, Jacqueline Marchand-Brynaert<sup>c</sup>, Yves-Jacques Schneider<sup>c</sup>, Véronique Prétat<sup>a,\*</sup>

<sup>a</sup> Université Catholique de Louvain, Unité de Pharmacie Galénique, Avenue E. Mounier, 73-20, 1200 Brussels, Belgium

<sup>b</sup> Institut des Sciences de la Vie, Université catholique de Louvain, Laboratoire de Biochimie cellulaire, Croix du Sud, 5, 1348 Louvain-La-Neuve, Belgium

<sup>c</sup> Université Catholique de Louvain, Unité de Chimie Organique et Médicinale, bâtiment Lavoisier, place Louis Pasteur, 1, 1348 Louvain-la-Neuve, Belgium

<sup>d</sup> Université de Liège, Centre d'Etude et de Recherche sur les Macromolécules, B6 Sart-Tilman, 4000 Liège, Belgium

<sup>e</sup> Department of Pathology, Cliniques Universitaires Saint-Luc, Université Catholique de Louvain, Avenue Hippocrate 10, 1200 Brussels, Belgium

Received 5 December 2006; accepted 30 April 2007

Available online 22 May 2007

## Abstract

To improve the efficiency of orally delivered vaccines, PEGylated PLGA-based nanoparticles displaying RGD molecules at their surface were designed to target human M cells. RGD grafting was performed by an original method called “photografting” which covalently linked RGD peptides mainly on the PEG moiety of the PCL–PEG, included in the formulation. First, three non-targeted formulations with size and zeta potential adapted to M cell uptake and stable in gastro-intestinal fluids, were developed. Their transport by an *in vitro* model of the human Follicle associated epithelium (co-cultures) was largely increased as compared to mono-cultures (Caco-2 cells). RGD-labelling of nanoparticles significantly increased their transport by co-cultures, due to interactions between the RGD ligand and the  $\beta_1$  integrins detected at the apical surface of co-cultures. *In vivo* studies demonstrated that RGD-labelled nanoparticles particularly concentrated in M cells. Finally, ovalbumin-loaded nanoparticles were orally administered to mice and induced an IgG response, attesting antigen ability to elicit an immune response after oral delivery.

© 2007 Elsevier B.V. All rights reserved.

**Keywords:** Nanoparticles; Oral vaccination; M cells targeting; RGD peptide

## 1. Introduction

Oral vaccination offers a large number of advantages compared to other routes of administration. It is a non-invasive, user-friendly method avoiding the need of sterile injection by qualified personnel. Nevertheless, oral administration of free vaccine often results in a very low immune response, which is mainly due to the premature degradation of the antigen in the gastrointestinal (GI) tract. Encapsulation of the vaccine in particulate systems became widely employed to solve this problem. It has been demonstrated that oral immunization with antigen-loaded microparticles induces mucosal IgA and systemic IgG antibodies responses, providing a complete immune response. Besides protecting the antigen against the harsh environment of the GI tract, nanocarriers are efficiently taken up

by M cells, key players of the mucosal immunity induction. In addition, biodegradable particles allow a sustained release of the antigen, increasing the duration of the contact between antigen and immune cells thus favouring an effective immune response [1–3].

Immune cells of the intestinal mucosa are mainly located in specialized structures called Peyer's patches (PPs). The Organized Mucosa Associated Lymphoid Tissue is separated from the lumen by the Follicle Associated Epithelium (FAE), composed of enterocytes and M cells. M cells are considered as the main entrance for pathogens to invade the body [3–7]. M cells are characterized by a disorganized brush border and a reduced mucus layer at their apical side. M cell basolateral membrane is deeply invaginated forming a pocket hosting lymphocytes. The characteristics of M cells makes them particularly adapted to antigen uptake: (i) by favouring antigen interactions with the apical membrane then optimizing antigen endocytosis, (ii) by shortening and facilitating antigen access to

\* Corresponding author. Tel.: +32 2 764 73 20; fax: +32 2 764 73 98.

E-mail address: [preat@farg.ucl.ac.be](mailto:preat@farg.ucl.ac.be) (V. Prétat).

the basolateral compartment, and thus (iii) by favouring quick and straightforward interactions between immune cells and antigen presenting cells (APC) present at the basal side.

The aim of this study was to target M cells with a specific ligand grafted on antigen-loaded PEGylated PLGA-based nanoparticles. Nanoparticles are known to be better taken up by M cells than microparticles [8–11]. Poly(lactide-co-glycolide) (PLGA) was chosen for its biodegradability properties, its biocompatibility and its approval by FDA. Poly( $\epsilon$ -caprolactone-co-ethylene glycol) (PCL-PEG), an amphiphilic copolymer, was added to the formulations (i) to take advantage of PEG repulsive properties to provide a higher stability of nanoparticles in biological fluids [12,13], (ii) to promote uptake by M cells in vitro [14], and (iii) to allow the grafting of a molecule targeting M cells on the surface of the nanoparticles. Three non-targeted formulations were first developed, composed of various percentages of PLGA, PLGA-PEG and PCL-PEG and encapsulating ovalbumin, as model antigen. Formulations were physicochemically characterized and their stability in biological media was evaluated. Their transport by M cells in vitro was studied and compared to enterocyte transport. Formulations were then targeted to  $\beta_1$  integrins expressed at the apical side of M cells [15,16] via an RGD peptide. A novel photografting method was developed to graft the peptide on PEG chain of PCL-PEG. The transport of targeted and non-targeted nanoparticles across M cells model was measured in vitro. The immune response induced by their oral delivery potential was also evaluated.

## 2. Materials and methods

### 2.1. Polymers synthesis and characterization

Tin(II) octanoate and  $\epsilon$ -caprolactone were purchased from Aldrich and purified just before use. Monomethoxy poly(ethylene glycol), triethylaluminum (1.9 M in toluene), and *N,N'*-dicyclohexylcarbodiimide (Aldrich) were used as received. D,L-lactide and glycolide were obtained from Purac and were purified and dried. Fluorescein (Sigma) and 4-(dimethylamino)pyridine (Fluka) were used as received.

PLGA was prepared by copolymerization of lactide and glycolide promoted by the dibutyltin dimethoxide (Aldrich) as catalyst as reported by Kricheldorf et al. [17]. To obtain fluorescent polymer, fluorescein with a carboxylic acid function prepared according to the method described by Cao et al. [18] was coupled to the MeO-PLGA-OH using *N,N'*-dicyclohexylcarbodiimide as coupling agent and 4-(dimethylamino)pyridine as catalyst. Synthesis of the PEG-PLGA copolymer was performed by ring-opening copolymerization of D,L-lactide and glycolide using PEG (Mn=4600, polydispersity=1.1) as macroinitiator and stannous octanoate as catalyst [19]. The PEG-PCL copolymer was also synthesized by ring-opening polymerization using triethylaluminum as catalyst [20].

$^1\text{H}$  NMR (400 MHz) spectra were recorded in  $\text{CDCl}_3$  at 25 °C with a Bruker AM 400 apparatus. Size-exclusion chromatography (SEC) was carried out in THF at a flow rate of 1 mL/min at 45 °C using a SFD S5200 auto-sampler liquid chromatograph equipped with a SFD refractometer index detector 2000 and

columns PL gel 5  $\mu\text{m}$  (columns porosity: 102, 103, 104, 105 Å). Polystyrene standards were used for calibration.

### 2.2. Preparation and characterization of PLGA-based nanoparticles

Nanoparticles were prepared by the “water-in-oil-in-water” solvent evaporation method, also called double emulsion method, as reported by Vila et al. [21], with modifications. Briefly, 50  $\mu\text{L}$  of a 5 mg/mL (PBS) ovalbumin (Sigma) solution were emulsified with 1 mL of methylene dichloride (Acros Organics) containing 50 mg of polymers (PLGA, PLGA-PEG and PCL-PEG) with an ultrasonic processor (70 W, 15 s). The second emulsion was performed with 2 mL of 1% sodium cholate (Sigma) aqueous solution, using an ultrasonic processor in the same conditions. The double emulsion was then poured drip into 100 mL of a 0.3% sodium cholate aqueous solution, and stirred at 37 °C during 45 min to evaporate the methylene dichloride. The nanoparticle suspension was then washed twice in PBS by centrifugation at 22000 g for 1 h to eliminate the excess of sodium cholate. Fluorescent nanoparticles were prepared by incorporating PLGA-FITC instead of PLGA in the formulations.

Nanoparticle size and zeta potential were determined using the Zetasizer Nano Series (Malvern).

### 2.3. Ovalbumin encapsulation efficiency

#### 2.3.1. [ $^3\text{H}$ ] radiolabelling of ovalbumin

Sodium boro[ $^3\text{H}$ ]hydride (100 mCi) was supplied by Amersham Biosciences. Radiolabelling of ovalbumin (Sigma) was performed by reductive alkylation of amino groups as previously described [22]. The [ $^3\text{H}$ ] ovalbumin specific activity was obtained by measuring the total protein concentration by Bradford test, according to the manufacturer's instructions, and the radioactivity by liquid scintillation. The peptide integrity after labelling was demonstrated by autoradiography (Hyperfilm, Amersham Biosciences) after SDS-PAGE electrophoresis (11% (w/v) of polyacrylamide gel), Tris-glycine running buffer (192 mM Tris, 25 mM Tricine, 0.1% (w/v) SDS) (data not shown).

#### 2.3.2. Encapsulation efficiency

$^3\text{H}$  radiolabelled ovalbumin was used to determine encapsulation efficiency. 100  $\mu\text{L}$  of the supernatants, obtained during nanoparticle washing (centrifugation) and 100  $\mu\text{L}$  of nanoparticles were dissolved in Aqualuma (Lumac\*LSC) and processed on a liquid scintillation counter (Liquid Scintillation Counter, Wallac 1410, Amersham Bioscience). Encapsulation efficiency was expressed as the percentage of ovalbumin encapsulated in nanoparticles compared to the initial amount of ovalbumin included in the formulation. Protein content in the supernatant was also measured by microBCA Protein assay Kit (Pierce PERBIO).

### 2.4. Nanoparticle stability studies in biological fluids

$^3\text{H}$  ovalbumin-loaded nanoparticles (50  $\mu\text{L}$ , 2 mg of polymer) were incubated in 500  $\mu\text{L}$  of HCl (0.1 N), mimicking

gastric environment, and incubated at 37 °C under gentle mechanic stirring. Nanoparticle size (Zetasizer Nano Series Malvern) and ovalbumin released were monitored over time. At various time intervals, nanoparticle suspensions were centrifuged at 22,000 g during 45 min. Radioactivity in the supernatant and the nanoparticles was measured by liquid scintillation counting, to measure the amount of ovalbumin released.

The same protocol was followed to determine the nanoparticle stability in Fasted State Simulated Intestinal Fluid (FaSSIF) [23] composed of  $\text{KH}_2\text{PO}_4$  (22.4 mM), NaOH (pH 6.5), sodium taurocholate (3 mM), lecithin (0.75 mM), KCl (0.1 M).

## 2.5. Nanoparticle transport across the *in vitro* M cells model

### 2.5.1. Cell lines and culture media

Human colon carcinoma Caco-2 line (clone 1), obtained from Dr. Maria Rescigno, University of Milano-Bicocca, Milano (IT) [24], from passage  $x+12$  to  $x+30$ , and human Burkitt's lymphoma Raji B line (American Type Culture Collection) from passage 102 to 110 were used.

### 2.5.2. *In vitro* model of the human FAE

Caco-2 cells and Raji cells were grown as previously described [8,14,15,25]. The inverted *in vitro* model of the human FAE was obtained as described by des Rieux et al. [25]. Briefly, 3–5 days after Caco-2 cell seeding, the inserts (Transwell® polycarbonate inserts (12 wells, pore diameter of 3  $\mu\text{m}$ , polycarbonate) purchased from Corning Costar) were inverted, placed in Petri dishes filled with supplemented DMEM+1% (v/v) penicillin–streptomycin and a piece of silicon tube was placed on each insert basolateral side. Inverted cells were cultivated for 9–11 days and the basolateral medium was changed every other day. Then, Raji cells were added in the basolateral compartments of inserts. The co-cultures were maintained for 5 days. Mono-cultures of Caco-2 cells, cultivated as above but without the Raji cells, were used as controls. Before the experiments, the silicon tubes were removed and the cell monolayers placed in multiwell plates and washed twice in HBSS. Inserts were used in their original orientation for all the following *in vitro* experiments. Cell monolayer integrity, both in co- and mono-cultures, was controlled by transepithelial electrical resistance (TEER) measurement.

### 2.5.3. Transport experiments

Transport experiments were run in HBSS at 37 °C. Nanoparticle concentration was adjusted by diluting the stock solution (checked by FACS analysis) in HBSS to a final concentration of  $2.7 \cdot 10^{10}$  nanoparticles/mL. After equilibration in HBSS at 37 °C, the apical medium of the cell monolayers was replaced by a nanoparticle suspension (400  $\mu\text{L}$ ) and inserts were incubated at 37 °C during 90 min. Basolateral solutions were then sampled and the number of transported nanoparticles was measured using a flow cytometer (FACScan, Becton Dickinson) [8,15]. Results are expressed as apparent permeability coefficient

(Papp) [26], as a mean  $\pm$  standard error of the mean (SEM). The Papp is defined by the following formula:

$$\text{Papp} = \frac{dQ}{dtAC_0}$$

$dQ/dt$	amount of product present in the basal compartment in function of time (nb/s)
$A$	area of transwell ( $\text{cm}^2$ )
$C_0$	initial concentration of product in apical compartment (nb/mL)

Cell monolayers were also apically pre-incubated with anti- $\beta_1$  integrin at 5  $\mu\text{g}/\text{mL}$  in HBSS for 1 h at 37 °C, before adding nanoparticle suspensions (formulation C with and without RGD-labelling) at a final concentration of  $2.7 \cdot 10^9$  nanoparticles/mL. The inhibitor was present throughout the whole transport experiment (90 min at 37 °C).

Since transport of carboxylated polystyrene nanoparticles (Molecular Probes) (model nanoparticles) has been well characterized [8,15,25], these nanoparticles were used as control of the *in vitro* model functionality. The absence of cytotoxicity of the different formulations was assessed by measuring the lactate dehydrogenase (LDH) activity released from the cytosol of damaged cells into the apical medium (BioGene™ Kit).

## 2.6. $\beta_1$ and $\alpha_5\beta_1$ integrin expression on the apical side of the M-like cells

Inserts were fixed in 4% (v/v) formalin, and then cut with a razor blade into thin sheets that were placed in Agar gel and embedded in paraffin. Thick, 5  $\mu\text{m}$ , sections were cut and, after paraffin removal by xylene, were rehydrated and boiled for 75 min in 10 mM citrate buffer 0.05% (v/v) Triton X-100, pH 5.8 with a water bath. Endogenous peroxidase activity was blocked by incubating in 0.3% (v/v)  $\text{H}_2\text{O}_2$  for 30 min and non-specific antibody staining was prevented by preincubation in 10% (v/v) normal goat serum for 30 min. Sections were then incubated either with anti  $\beta_1$  integrin monoclonal antibody (1/50 dilution) (USBiological) or with anti  $\alpha_5\beta_1$  integrin monoclonal antibody (1/300) (CD29 from BioGenex), at room temperature overnight and revealed using the Envision system (Dako) with diaminobenzidine (Sigma-Aldrich). Finally, samples were mounted and examined with an AxioVision 3.1 microscope (Zeiss) equipped with an AxioCam HRc digital camera (Zeiss).

## 2.7. Synthesis of PCL-PEG-g-GRGDS by photografting

PCL-PEG (15200-4600) or PCL-PEG (21200-6000) (for XPS studies) was solubilized in methylene dichloride with *O*-succinimidyl 4-(*p*-azidophenyl) butanoate [27] (0.2 to 0.6 mmol per gram of PCL-PEG). After solvent evaporation, the sample (shavings) was irradiated at 254 nm in a quartz flask under argon atmosphere for 20 min. After washing with isopropanol: ethyl acetate (19: 1, v/v) the activated sample was immersed in a 1 mM solution of GRGDS (GRGDS (97.0%) NeoMPS) (0.5 mg/mL) in phosphate buffer (0.1 M):acetonitrile (1: 1, v/v) at pH 8 and

shaked for 24 h at 20 °C. The sample was washed 3 times with 5 mM HCl and 5 times with water, shacked overnight in water, rinsed with methanol and dried under vacuum at 40 °C to constant weight. The blank sample was prepared following the same protocol but omitting the azide reagent.

The XPS analyses were performed on a Kratos Axis Ultra spectrometer (Kratos Analytical) equipped with a monochromatised aluminium X-ray source (powered at 10 mA and 15 kV). Data treatments were done with the CasaXPS program (Casa Software) with a Gaussian/Lorentzian (70/30) product function and after subtraction of a linear baseline. The copolymer samples were casted, from solvent evaporation, on glass plates that were fixed on a stainless steel multispecimen holder by using double-sided conductive tape. The nanoparticles powders were pressed into small stainless steel troughs mounted on a multi specimen holder.

### 2.8. Oral immunization with ovalbumin-loaded nanoparticles

Specific pathogen-free female NMRI mice aged 6–8 weeks were purchased from the animal facility of the Université Catholique de Louvain. The mice were kept in hanging wire cages and allowed to feed and drink ad libitum. The Ethical Committee for Animal Care of the Université Catholique de Louvain has approved the in vivo protocols.

Female NMRI mice (eight per group) were immunized by gastric gavage or intramuscular injection (positive control group). One group received by gavage ovalbumin in PBS (5 µg/100 µL), while six groups were intragastrically fed with various formulations (formulations A, B, C with or without the GRGDS ligand) (100 µL of nanoparticles containing 5 µg of ovalbumin). Another group received two intramuscular injections of 50 µL of ovalbumin in each quadriceps (5 µg/100 µL) at day 0. 14 and 28 days after the first immunization, mice were boosted with the same gavage or injection. Mice were fasted the day before their immunization. Blood samples were collected by retro-orbital puncture on weeks 2, 4, 6, 10 and 12. Sera isolated by centrifugation (3000 rpm during 20 min at 4 °C), were stored at –20 °C before analysis. Ovalbumin-specific IgG levels were evaluated by enzyme-linked immunosorbent assay (ELISA) [28]. Sera dilutions were made in ovalbumin-coated plates (Nunc-Immuno Plate F96 MAXISORP) and detection of anti-ovalbumin antibodies was carried out using peroxidase-labelled rat anti-mouse immunoglobulin G (total IgG) (LO-IMEX). Titers were defined as the logarithm of the highest dilution giving an optical density of 0.2 at 450 nm (detection limit: 0.7). For cytokine assays, mice were sacrificed, and their spleen were removed aseptically. Splenocytes were adjusted to a concentration of  $5 \times 10^6$  cells/mL and cultured 500 µl per well in 48-well tissue culture plates in RPMI 1640 medium supplemented with 10% foetal bovine serum, 1% penicillin/streptomycin, 1% sodium pyruvate,  $5 \times 10^{-5}$  M 2-mercapto-ethanol and 10% MEM (In vitrogen, Belgium). Cells were stimulated by the addition of 10 µg of ovalbumine per well. Unstimulated cells were used as control. Cell supernatants were collected either after 48 h for interferon-gamma (IFN-g) assay or after 72 h for interleukin-4 (IL-4) assay. Cytokine concentrations in the supernatants were measured using mouse IFN-g and IL-4 DuoSet ELISA development kits (R&D

Systems Europe Ltd, Abingdon, UK) according to the manufacturer's protocols.

### 2.9. In vivo localization of nanoparticles in mouse Peyer's patches by confocal microscopy

Female NMRI mice (2 per condition), 6–8 weeks old, were fasted overnight and supplied with water ad libitum before the experiment. FITC-labelled nanoparticles grafted or not with the GRGDS ligand (200 µL of nanoparticles, 30 mg of polymer) were intragastrically administered. Three hours after the gavage, mice were euthanized by cervical dislocation. Two Peyer's patches by mouse were excised, washed with PBS and fixed in cold methanol at –20 °C for 45 min. Then, tissues were rinsed in PBS (3 times) and incubated for 60 min at room temperature with 10 µg/mL of rhodamine labelled UEA-1 lectin (VECTOR Laboratories) [29]. Tissues were then washed 5 times in PBS and placed into "chambered coverglass system" (Lab-Tek®II — Nalgen Nunc International) for confocal laser scanning microscopy (CLSM) (Axiovert 135 M microscope equipped with a Bio-Rad MRC1024 confocal system) observation. Non-Peyer's patch tissues were used as control.

### 2.10. Statistics

Statistical analysis of the results was assessed by using the JMP4 software. Data were first tested for log normal distribution and homogeneity of variances and then analysed by one way ANOVA.  $p$  value < 0.05 were considered as significant.

## 3. Results

### 3.1. Polymer characterization

Polymers (PLGA, PLGA–PEG and PCL–PEG) were characterized by NMR spectroscopy and SEC (Table 1). Their molecular weight was in the range of 25,000 g/mol. The SEC analysis of the amphiphilic copolymers confirmed that all the macroinitiator has initiated polymerization, leading to the formation of the diblock copolymers, free of homopolymers.

Table 1  
Chemical description of the polymers included in the formulations

Polymer	Mn (SEC) <sup>a</sup> g/mol	Mn (NMR) g/mol <sup>b</sup>	mol.% glycolide	Polydispersity index <sup>c</sup>
PLGA	22,000		25	1.8
Fluorescent PLGA	23,600		29	1.6
PEG-b-PLGA	29,300	4600–16,500(L)/ 4700(G)	26	1.7
PCL-b-PEG	22,400	4600–15,200		1.15
PCL-b-PEG	26,300	6000–21,200		1.15

<sup>a</sup> Polystyrene calibration.

<sup>b</sup> Determined by NMR by the following formula:  $(I_{4.7}/2)/(I_{5.2} + (I_{4.7}/2)) \times 100$ , where  $I_{4.7}$  is the signal intensity of the glycolide unit at 4.7 ppm ( $\text{CH}_2\text{OC}=\text{O}$ ) and  $I_{5.2}$  is the signal intensity of the lactide unit at 5.2 ppm ( $\text{CH}(\text{CH}_3)\text{OC}=\text{O}$ ).

<sup>c</sup> PDI = Mw/Mn, determined by SEC by polystyrene standard.



Table 2  
Composition (% w) of the investigated formulations

	PLGA 22,000	PLGA-PEG 21,000–5000	PCL-PEG 15,000–5000
Formulation A	50		50
Formulation B	45	45	10
Formulation C	70	15	15

The coupling reaction of FITC on PLGA was achieved under mild conditions to avoid polymer degradation, which was confirmed by SEC (data not shown). The achievement of the fluorescein grafting on PLGA was assessed by SEC using a UV–VIS detector (data not shown). The reaction yield was calculated by NMR to be 75%.

### 3.2. Physicochemical characterization of the nanoparticles

Nanoparticles were composed of PLGA, a biodegradable and FDA approved polymer which formed the core of the nanocarriers. An amphiphilic copolymer containing PEG was added to the formulation to stabilize the nanoparticles [12–13] to promote uptake by M cells [14] and to allow targeting by grafting ligands on the PEG moiety. Three formulations containing PLGA, PLGA-PEG and PCL-PEG were investigated. Their composition is reported in Table 2. As grafting on PLGA-PEG was difficult due to chemical instability, PCL-PEG was selected for photografting of M cell ligands. Taking into account the previous results of our group, we chose to investigate formulations with about 50% of PEG [14]. The binary formulation A was simply composed of PLGA and PCL-PEG in equal proportion. To improve the size homogeneity and stability of the nanoparticles, PLGA-PEG was added to the formulation. Different proportions of PLGA-PEG and PCL-PEG were investigated (data not shown). The formulation B composed of 10% of PCL-PEG and 45% of PLGA-PEG was selected because of its lower size polydispersity. Lastly, formulation C, containing only 30% of total PEG (against 50–55% for the two others), was tested. The hypothesis was that a weaker sterical hindrance at the particle surface might be more appropriate to expose the targeting ligand.

#### 3.2.1. Physicochemical properties of the formulations

Formulations A, B and C were characterized in term of size, zeta potential and ovalbumin encapsulation efficiency (Table 3). They all had a mean size around 200 nm which is commonly considered as optimal size for nanoparticles to be taken up by

Table 3  
Physicochemical properties of the nanoparticles ( $n=3$  to 5)

	Formulation A	Formulation B	Formulation C	Formulation C RGD
Size (nm)	208±20	200±22.5	201±24	211±2.89
Size polydispersity index	0.152	0.166	0.170	0.169
Zeta potential (mV)	-6.6±1.2	-6.8±4.2	-9.1±5.8	-13.8±4.3
Encapsulation efficiency (%)	50±6	30±2	40±1	40

PPs [8]. Besides, the small polydispersity index indicated that nanoparticle populations were homogeneous. Moreover, the zeta potentials of the three formulation were close to neutrality, most probably because of the presence of PEG chains shielding negative charges present at the nanoparticle surface. Finally, ovalbumin was efficiently encapsulated (30 to 50%).

#### 3.2.2. Nanoparticle stability in biological media

To check if the nanocarriers could protect the antigen until it reaches M cells in the gastro-intestinal tract, the stability of [ $^3\text{H}$ ] ovalbumin-loaded nanoparticles was investigated upon incubation in different simulated biological fluids: HCl 0.1 N which mimics gastric conditions and FaSSIF for intestinal environment (Fig. 1). After 2 h of incubation in HCl 0.1 N, less than 5% of the [ $^3\text{H}$ ] labelled ovalbumin were recovered in the supernatants after centrifugation of the nanoparticle suspension, which is consistent with nanoparticle size stability in gastric conditions. After 6 h of incubation in FaSSIF, nanoparticle size was not altered. A slight release of [ $^3\text{H}$ ] labelled ovalbumin, less than 10% during the duration of the experiment, was observed for the formulations B and C. However, a burst effect was observed for the formulation A. 20% of [ $^3\text{H}$ ] labelled ovalbumin was released during the first hour of incubation, and this amount remained stable during all the experiment. The stability of RGD-labelled nanoparticles was also demonstrated (data not shown). Hence, the three formulations are adapted to

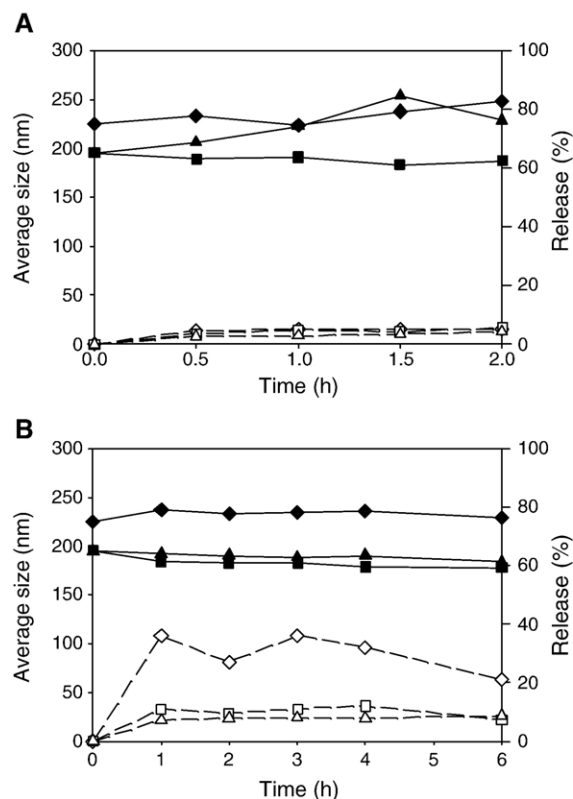


Fig. 1. Evolution of the nanoparticle size (close symbols) and  $^3\text{H}$  ovalbumin release (open symbols) during incubation in A) HCl 0.1 N and B) FaSSIF for formulations A (PLGA/PCL-PEG 50:50) ( $\diamond$ ), B (PLGA/PLGA-PEG/PCL-PEG 45:45:10) ( $\square$ ), and C (PLGA/PLGA-PEG/PCL-PEG 70:15:15) ( $\triangle$ ) ( $n=3$ , CV < 10%).

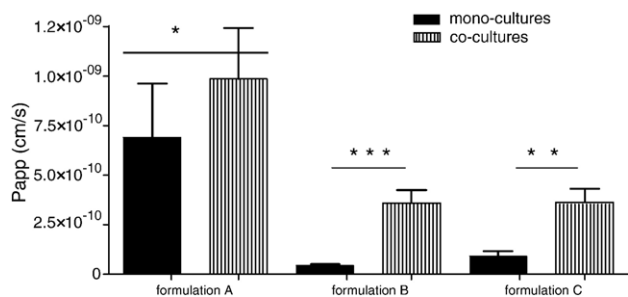


Fig. 2. Comparison of the transport of the different formulations across mono- and co-cultures.  $2.7 \cdot 10^{10}$  nanoparticles/ml of formulation A (PLGA/PCL-PEG 50:50), B (PLGA/PLGA-PEG/PCL-PEG 45:45:10) and C (PLGA/PLGA-PEG/PCL-PEG 70:15:15), suspended in HBSS were added to the apical pole of the cell monolayers. Mono- and co-cultures were incubated for 90 min at 37 °C ( $n=20-27$ ). The number of transported nanoparticles was evaluated by flow cytometry and is expressed as apparent permeability coefficient (Papp) as a mean  $\pm$  standard error of the mean (SEM) \* $p < 0.05$ , \*\* $p < 0.01$ , \*\*\* $p < 0.001$ .

the oral route of administration: ovalbumin remains inside the nanocarrier in gastro-intestinal simulated fluids.

### 3.3. In vitro transport of nanoparticles by enterocytes or M cells

In order to evaluate the formulation transport by M cells, the in vitro model of the human FAE, previously described by des Rieux et al., was used [25]. The nanoparticle transport by co-cultures (Caco-2 and Raji cells) was compared to the transport by mono-cultures (Caco-2 cells) (Fig. 2). Formulation A transport was high but not significantly different on mono- or co-cultures, attesting that the transport was not M cell specific. Nanoparticle transport was 4-fold (formulation C ( $p < 0.01$ )) and 10-fold (formulation B ( $p < 0.001$ )) increased by co-cultures as compared to mono-cultures. Whatever the formulation, LDH activity in apical medium was similar to the negative control (HBSS,  $< 5\%$ ). TEER measurements before and after the experiments confirmed that the nanoparticles were not cytotoxic at the concentration investigated (data not shown).

### 3.4. Apical expression of $\beta_1$ and $\alpha_5\beta_1$ integrins in the M-like cell model

In order to find M cells specific ligands, immunohistochemistry was led on the human FAE model. It has been previously reported that  $\beta_1$  integrins were present at the apical surface of M cells [15,16,30]. Fig. 3 illustrates that in vitro, conversion of Caco-2 cells to M cells could be characterized by the expression of  $\beta_1$  and  $\alpha_5\beta_1$  integrins at the apical surface of the co-cultures. Hence, RGD, the universal peptide recognizing integrins [31], was chosen as a ligand for human M cells.

### 3.5. Synthesis and characterization of the PCL-PEG-g-GRGDS

To display the RGD ligand at the surface of the nanoparticles, a novel photografting method was developed to graft the peptide mainly on the PEG moiety of PCL-PEG. This covalent coupling of GRGDS peptides required first the derivatization of the native

copolymer PCL-PEG with reactive functions susceptible to react with the peptide terminal free amines. We chose to introduce *N*-hydroxysuccinimidyl (NHS) esters via a photochemical process using *O*-succinimidyl 4-(*p*-azidophenyl) butanoate as a crosslinking reagent [27,32]. Under UV irradiation, this molecule generates highly reactive nitrenes able to make insertion reactions into C-H bonds of the copolymer matrix, while the NHS functions remain unchanged. NHS-activated PCL-PEG was then immersed into a 1 mM solution of the peptide for 24 h, then appropriately washed and dried. The resulting PCL-PEG-g-GRGDS was analyzed by X-Ray Photoelectron Spectroscopy (XPS) [33]:

PCL-PEG-g-GRGDS: O 1s (22.65 %), N 1s (0.98 %), C 1s (73.66%), Si 2p (2.71%);

PCL-PEG: O 1s (23.69 %), C 1s (71.54 %), Si 2p (4.78%).

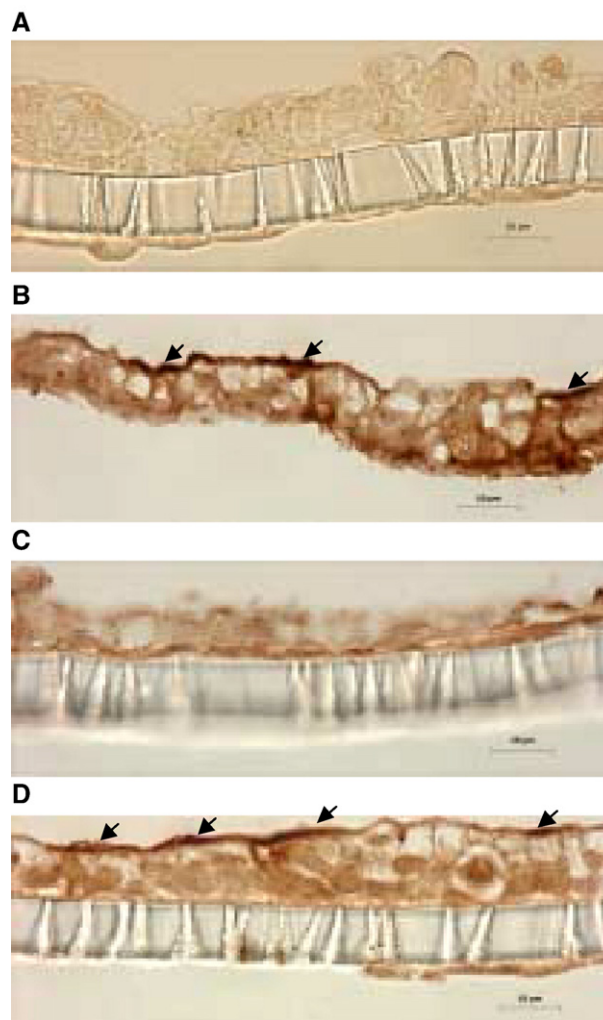


Fig. 3. Apical expression of  $\beta_1$  and  $\alpha_5\beta_1$  integrins by M cells. Mono- and co-cultures were fixed and were placed in agar gel. 5  $\mu$ m thick paraffin sections were cut and used for immunohistochemistry. Sections were incubated with the anti  $\beta_1$  integrin monoclonal antibody (1/50) (A and B) while others were incubated with the anti  $\alpha_5\beta_1$  integrin monoclonal antibody (1/300) (C and D). Mono-cultures were used as controls (A,C). Cells positive for  $\beta_1$  and  $\alpha_5\beta_1$  integrins are indicated by arrows. \*The preparation of the samples can induce a detachment of the filter from the cell monolayer.

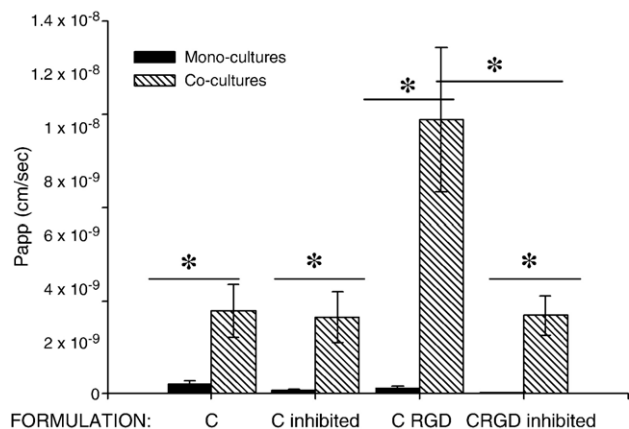


Fig. 4. Influence of RGD grafting on nanoparticle transport across mono- and co-cultures. Cell monolayers were first apically pre-incubated with anti- $\beta_1$  integrin at 5  $\mu\text{g}/\text{ml}$  in HBSS for 1 h at 37 °C, before adding nanoparticle suspension at a final concentration of  $2.7 \cdot 10^9$  nanoparticles/ml ( $n=11-16$ ). The number of transported nanoparticles was evaluated by flow cytometry and is expressed as apparent permeability coefficient (Papp) as a mean  $\pm$  standard error of the mean (SEM) \* $p < 0.05$ .

The surface atomic composition of this material revealed the presence of nitrogen atoms ( $\text{N1s}/\text{C1s}=1.33 \cdot 10^{-2}$ ), whereas no N1s peak could be detected on the blank sample (PCL-PEG similarly treated, but in the absence of crosslinking reagent). These results confirmed the grafting of GRGDS.

### 3.6. Physicochemical characterization of RGD-labelled nanoparticles

Formulation C (PLGA/PLGA-PEG/PCL-PEG 70:15:15) was chosen to study the effect of the RGD sequence grafting at nanoparticle surface on M cell targeting. First, it has been verified that the presence of the ligand on the PCL-PEG did not change the physicochemical properties of the nanoparticles. Table 3 demonstrates that except a slight increase of nanoparticle size, encapsulation efficiency, zeta potential and size polydispersity remained unchanged. Stability of the RGD-labelled formulation C in biological simulated fluids was also investigated. Incubation in HCl or FaSSIF did not affect nanoparticle size and no release of ovalbumin was observed (data not shown).

To investigate the chemical composition of the nanoparticle surface, and especially, to confirm the presence of the ligand GRGDS, XPS was carried on freeze-dried nanoparticles, looking more precisely for N1s peak [12,34]:

GRGDS-NP: Na 1s (1.29%), O 1s (31.50 %), N 1s (0.16%), C 1s (63.70%), Cl 2p (2.08%), Si 2p (1.28%)

Blank-NP: Na 1s (2.42%), O 1s (31.80 %), C 1s (60.40%), Cl 2p (4.10%), Si 2p (1.28%).

Since nitrogen atoms were detected on the surface of nanoparticles containing PCL-PEG-GRGDS ( $\text{N1s}/\text{C1s}=0.25 \cdot 10^{-2}$ ) but not on the surface of non-targeted blank nanoparticles, the

nitrogen signals were very likely due to covalently immobilized GRGDS peptides located at the nanoparticle surface and well displayed to target  $\beta_1$  integrins. These results were confirmed with the detection of a perfluorated probe grafted by the same method [33].

### 3.7. In vitro transport of the RGD-labelled formulation by enterocytes and M cells

In order to evaluate the influence of the ligand at the nanoparticle surface on their transport by M cells, formulations C, with or without GRGDS, were incubated on the apical side of the co-cultures and mono-cultures, at 37 °C, during 90 min. The presence of the PCL-PEG-GRGDS in the formulation increased the transport of nanoparticles across the M cell model, with a factor of 3.5 ( $p < 0.05$ ) compared to the non-targeted formulation (Fig. 4). On the contrary, no significant difference between the uptake of RGD-targeted and “naked” formulations was observed on the monocultures. To confirm that RGD grafting allows a specific targeting of M cells, an anti-integrin  $\beta_1$  antibody was added to the apical medium. The transport of the RGD-targeted nanoparticles in co-culture was inhibited ( $p < 0.05$ ) and reached the value of non-targeted nanoparticle transport. These data indicate that the GRGDS, exposed at the nanoparticle surface, can interact with M cell integrins, leading to an improvement in the transport by these cells.

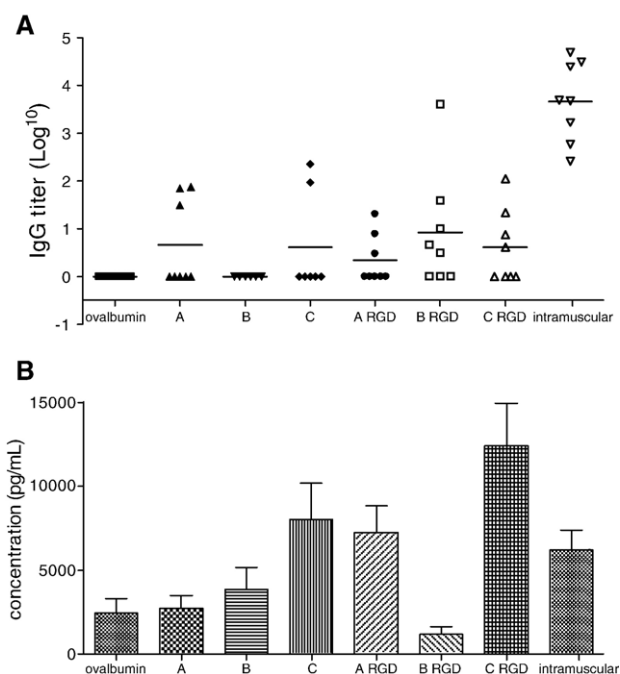


Fig. 5. Influence of the formulation composition on (A) IgG titers in serum and (B) IFN $\gamma$  production by splenocytes. Mice were fed with ovalbumin solution (PBS); formulation A (PLGA/PCL-PEG 50:50); formulation B (PLGA/PLGA-PEG/PCL-PEG 45:45:10); formulation C (PLGA/PLGA-PEG/PCL-PEG 70:15:15). Intramuscular injection was used as positive control. A) Mice individual IgG titers 10 weeks after the first immunization ( $n=7-8$ ). B) IFN $\gamma$  production by splenocytes 13 weeks after the first immunization (4 mice; 3 wells).



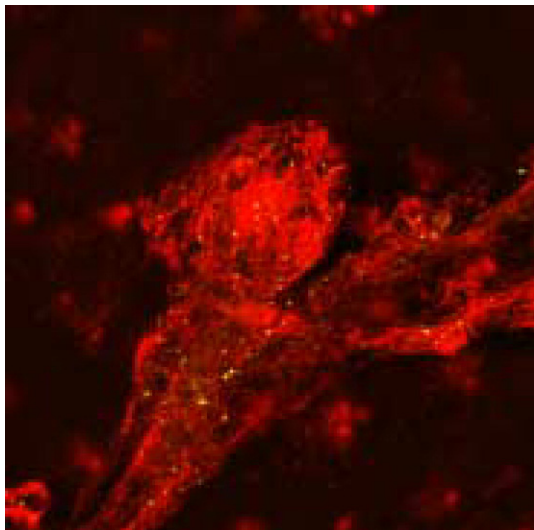


Fig. 6. CLSM visualization of Peyer's patches, demonstrating the uptake of FITC-PLGA nanoparticles by the FAE in mice fed with targeted formulation C (FITC-PLGA/PLGA-PEG/PCL-PEG-GRGDS 70:30:30). M cells were stained with rhodamin-labelled UEA-1 Lectin (10  $\mu\text{g}/\text{mL}$ ). Bar: 50  $\mu\text{m}$ .

### 3.8. Oral immunization with ovalbumin-loaded nanoparticles

In order to evaluate the formulations as vaccine oral delivery systems, an immunization experiment was performed on mice, using 5  $\mu\text{g}$  ovalbumin as model antigen. The IgG titers of each mouse detected 10 weeks after priming are displayed in Fig. 5A. IgG were detected in 3, 0 and 2 mice out of 8 after oral administration of the nanoparticle formulation A, B and C respectively. Even if the mean production of IgG was not increased with targeting, the number of mice producing IgG was slightly higher in the case of immunization with targeted formulations compared to non-targeted ones (3, 5 and 4 out of 8 mice after oral administration of the RGD-labelled nanoparticle formulation A, B and C respectively).

As expected, IgG were not detectable in the sera of mice fed with free ovalbumin, emphasizing the role of antigen encapsulation in nanocarriers to protect it. The intramuscular route remained the most efficient one, providing high levels of IgG (IgG titer=2 to 4.4). Every mouse treated with ovalbumin via the intramuscular route presented IgG in their serum, which was not the case upon oral immunization with nanoparticles. However, it is worth noticing that a small amount of ovalbumin (5  $\mu\text{g}$ ) did induce an immune response in the groups immunized orally with nanoparticles.

The cellular response was also investigated. The IL4 production by splenocytes remained very low (<30 pg/ml, data not shown). Significant IFN $\gamma$  production was induced in some of the groups immunized orally (Welsh's test indicates statistical difference between the groups).

### 3.9. Uptake of targeted nanoparticles in mouse Peyer's patches

Fluorescent nanoparticles, precisely formulation C with or without GRGDS, were administered to fasted mice by oral

gavage. The location of these nanoparticles in the gut was investigated by confocal microscopy. Fig. 6 reveals that targeted nanoparticles were localized mainly in the PPs and that they were often co-localized with M cells (stained with rhodamine labelled UEA-1 Lectin). Very few nanoparticles were observed out of the PPs (data not shown). Non-targeted nanoparticles were less numerous in PPs and more scattered.

## 4. Discussion

Three different formulations, composed of various percentages of PLGA, PLGA-PEG and PCL-PEG, have been developed and tested as oral delivery systems of vaccine. They present good physicochemical properties for M cell uptake and are stable in gastrointestinal fluid, being then suitable for the oral route.

As the presence of  $\beta_1$  integrins on M cells [15,16] was confirmed *in vitro*, the RGD peptide was selected as a model targeting ligand to M cells. A novel photografting technique was developed to covalently bind the peptide GRGDS mostly to the PEG chain of PCL. The presence of the ligand at the surface of the nanoparticles was demonstrated by XPS.

This RGD ligand at the surface of the nanoparticles (formulation C) increased the transport of the nanoparticles across co-cultures *in vitro*. The specific targeting of the  $\beta_1$  integrins by the RGD-labelled nanoparticles was demonstrated in the co-cultures by the inhibition of their transport by anti- $\beta_1$  integrin. This result was not observed with formulation B (data not shown). This could be explained by a better accessibility of the ligand at the nanoparticle surface, due to the lower amount of PEG in the formulation C (30%) compared to the formulation B (55%). Besides, hydrophobic nanoparticles have been reported to be better transported by M cells than hydrophilic particles [35,36]. 30% of PEG in the formulation seemed enough to induce a shielding of the nanoparticle surface charges (zeta potential=-9 mV against -40 mV without PEG).

It is well accepted that nanoparticle surface properties are of utmost importance for their uptake by intestinal epithelial cells. A compromise between hydrophobicity/hydrophilicity, surface charge targeting and particle stabilization has to be found to develop the most appropriate vector [2]. Some bioadhesive and hydrophilic particles, made of chitosan for instance [37], are known to be largely taken up by enterocytes. So, two strategies of oral delivery coexist: targeting specifically M cells which are not numerous but specialized in particle endocytosis, or increasing the nanoparticle transport across enterocytes, which represent the main population of epithelial cells [2]. Targeting M cells is a very appealing strategy because the particular characteristics of these cells allow a rapid contact between antigens and APC and B lymphocytes.

The immunization with the nanoparticles elicited a humoral but also a cellular immune response attesting that the antigen was efficiently presented to T lymphocytes by the APC. Antigen loading in the nanoparticles allowed the use of a small amount of antigen: we used only 5  $\mu\text{g}$  of antigen, against 100  $\mu\text{g}$  and more in usual assays. This could be very likely explained by the protection of the antigen into the nanocarrier against



degradation in the gastrointestinal tract. Alternatively, the presentation of the antigen in a particulate form could elicit an immune response whereas a soluble protein antigen induces tolerance by the mucosal immune system [1]. This is very promising since human oral vaccine applications are still limited by the too high amounts of antigens required to elicit an efficient protection [38].

At last, we demonstrated that the use of a RGD ligand at the nanoparticle surface to target M cells provoked a slight increase in the number of mice producing IgG after immunization, thus confirming the importance of targeting the carriers. Nevertheless, no increase of the IgG production in serum was observed with the use of the RGD ligand. This could be due to a partial degradation of the peptide during its trafficking in the gastrointestinal tract. To avoid the ligand degradation in the stomach or in the gut, non-peptidic  $\beta_1$  integrin ligand could be used and grafted on the nanoparticles in the place of RGD peptides. The addition of a mucosal adjuvant in the formulation could also be explored [1].

## Acknowledgements

This work was supported by the DGTRE (Walloon region government) for the project VACCINOR (WINNOMAT). The Belgian FRSM (*Fonds de la Recherche Scientifique Médicale*) is also thanked for financial support.

The authors thank P. Vandersmissen and A. Tonon, both from the Ludwig Institute Cancer Research (Brussels, Belgium) for their help during confocal analyses and the FACScan analyses, respectively, S. Devouge for performing the XPS using the facilities of the Laboratoire de Chimie des Interfaces (Prof. P.G. Rouxhet and Ir. M.Genet, Université catholique de Louvain, Louvain-la-Neuve, Belgium); A. Vanderplaaschen (Université de Liège) for helpful discussion; M.-L. Vanderhaeghen and J.-P. Vandiest, both from the School of Pharmacy (Université catholique de Louvain, Brussels, Belgium) for their technical support.

## References

- [1] J. Mestecky, J. Bienenstock, M. Lamm, L. Mayer, J. McGhee, W. Strober, *Mucosal Immunity*, Elsevier academic Press, 2005.
- [2] A. des Rieux, V. Fievez, M. Garinot, Y.J. Schneider, V. Pr eat, Nanoparticles as potential oral delivery systems of proteins and vaccines: a mechanistic approach, *J. Control. Release* 116 (2006) 1–27.
- [3] D.J. Brayden, M.A. Jepson, A.W. Baird, Keynote review: intestinal Peyer's patch M cells and oral vaccine targeting, *Drug Discov. Today* 10 (2005) 1145–1157.
- [4] J.P. Kraehenbuhl, M.R. Neutra, Epithelial M cells: differentiation and function, *Annu. Rev. Cell. Dev. Biol.* 16 (2000) 301–332.
- [5] M.H. Jang, M.N. Kweon, K.I. Watani, M. Yamamoto, K. Terahara, C. Sasakawa, T. Suzuki, T. Nochi, Y. Yokota, P.D. Rennert, T. Hiroi, H. Tamagawa, H. Iijima, J. Kunisawa, Y. Yuki, H. Kiyono, Intestinal villous M cells: an antigen entry site in the mucosal epithelium, *Proc. Natl. Acad. Sci. U. S. A.* 101 (2004) 6110–6115.
- [6] M.R. Neutra, Current concepts in mucosal immunity. V role of M cells in transepithelial transport of antigens and pathogens to the mucosal immune system, *Am. J. Physiol.* 274 (1998) G785–G791.
- [7] A. Siebers, B.B. Finlay, M cells and the pathogenesis of mucosal and systemic infections, *Trends Microbiol.* 4 (1996) 22–29.
- [8] A. des Rieux, E.G.E. Ragnarsson, E. Gullberg, V. Pr eat, Y.J. Schneider, P. Artursson, Transport of nanoparticles across an in vitro model of the human intestinal follicle associated epithelium, *Eur. J. Pharm. Sci.* 25 (2005) 455–465.
- [9] M.P. Desai, V. Labhsetwar, G.L. Amidon, R.J. Levy, Gastrointestinal uptake of biodegradable microparticles: effect of particle size, *Pharm. Res.* 13 (1996) 1838–1845.
- [10] T. Jung, W. Kamm, A. Breitenbach, K.D. Hungerer, E. Hundt, T. Kissel, Tetanus toxoid loaded nanoparticles from sulfobutylated poly(vinyl alcohol)-graft-poly(lactide-co-glycolide): evaluation of antibody response after oral and nasal application in mice, *Pharm. Res.* 18 (2001) 352–360.
- [11] S. McClean, E. Prosser, E. Meehan, D. O'Malley, N. Clarke, Z. Ramtoola, D. Brayden, Binding and uptake of biodegradable poly-dl-lactide micro- and nanoparticles in intestinal epithelia, *Eur. J. Pharm. Sci.* 6 (1998) 153–163.
- [12] R. Gref, Y. Minamitake, M.T. Peracchia, V. Trubetskoy, V. Torchilin, R. Langer, Biodegradable long-circulating polymeric nanospheres, *Science* 263 (1994) 1600–1603.
- [13] C.A. Nguyen, E. Allemann, G. Schwach, E. Doelker, R. Gurny, Cell interaction studies of PLA–MePEG nanoparticles, *Int. J. Pharm.* 254 (2003) 69–72.
- [14] A. des Rieux, V. Fievez, M. Momtaz, C. Detrembleur, M. Alonso-Sande, J. Van Gelder, A. Cauvin, Y.-J. Schneider, V. Pr eat, Influence of M cells on oral delivery of helodermin, *J. Control. Release* 118 (2007) 294–302.
- [15] E. Gullberg, M. Leonard, J. Karlsson, A.M. Hopkins, D. Brayden, A.W. Baird, P. Artursson, Expression of specific markers and particle transport in a new human intestinal M-cell model, *Biochem. Biophys. Res. Commun.* 279 (2000) 808–813.
- [16] E. Gullberg, A.V. Keita, S.Y. Salim, M. Andersson, K.D. Caldwell, J.D. Soderholm, P. Artursson, Identification of cell adhesion molecules in the human follicle-associated epithelium that improve nanoparticle uptake into the Peyer's patches, *J. Pharmacol. Exp. Ther.* 319 (2006) 632–639.
- [17] H.R. Kricheldorf, J.M. Jonte, M. Berl, Polylactones. 3. Copolymerization of glycolide with l,l-lactide and other lactones, *Makromol. Chem.* 12 (1985) 25–38.
- [18] L.W. Cao, H. Wang, J.S. Li, H.S. Zhang, 6-Oxy-(N-succinimidyl acetate)-9-(2'-methoxycarbonyl)fluorescein as a new fluorescent labeling reagent for aliphatic amines in environmental and food samples using high-performance liquid chromatography, *J. Chromatogr. A.* 1063 (2005) 143–151.
- [19] M.L. Zweers, G.H. Engbers, D.W. Grijpma, J. Feijen, In vitro degradation of nanoparticles prepared from polymers based on dl-lactide, glycolide and poly(ethylene oxide), *J. Control. Release* 100 (2004) 347–356.
- [20] P. Vangeyte, R. J er ome, Amphiphilic block copolymers of high-molecular-weight poly(ethylene oxide) and either  $\epsilon$ -caprolactone or  $\gamma$ -methyl- $\epsilon$ -caprolactone: synthesis and characterization, *J. Pharmacol. Exp. Ther.* 42 (2004) 1132–1142.
- [21] A. Vila, H. Gill, O. McCallion, M.J. Alonso, Transport of PLA–PEG particles across the nasal mucosa: effect of particle size and PEG coating density, *J. Control. Release* 98 (2004) 231–244.
- [22] G.E. Means, R.E. Feeney, Reductive alkylation of amino groups in proteins, *Biochemistry* 6 (1968) 2192–2201.
- [23] J.B. Dressman, C. Reppas, In vitro–in vivo correlations for lipophilic, poorly water-soluble drugs, *Eur. J. Pharm. Sci.* 11 (2000) S73–S80.
- [24] M. Rescigno, M. Urbano, B. Valzasina, M. Francolini, G. Rotta, R. Bonasio, F. Granucci, J.P. Kraehenbuhl, P. Ricciardi-Castagnoli, Dendritic cells express tight junction proteins and penetrate gut epithelial monolayers to sample bacteria, *Nat. Immunol.* 2 (2001) 361–367.
- [25] A. des Rieux, V. Fievez, I. Th eate, J. Mast, V. Pr eat, Y.-J. Schneider, An improved in vitro model of human intestinal follicle-associated epithelium to study nanoparticle transport by M cells, *Eur. J. Pharm. Sci.* 30 (2007) 380–391.
- [26] P. Artursson, Epithelial transport of drugs in cell culture. I: a model for studying the passive diffusion of drugs over intestinal absorptive (Caco-2) cells, *J. Pharm. Sci.* 79 (1990) 476–482.
- [27] S. Devouge, C. Salvagnini, J. Marchand-Brynaert, A practical molecular clip for immobilization of receptors and biomolecules on devices' surface: synthesis, grafting protocol and analytical assay, *Bioorg. Med. Chem. Lett.* 15 (2005) 3252–3256.
- [28] C. Lombry, A. Marteleur, M. Arras, D. Lison, J. Louahed, J.C. Renauld, V. Preat, R. Vanbever, Local and systemic immune responses to intratracheal

- instillation of antigen and DNA vaccines in mice, *Pharm. Res.* 21 (2004) 127–135.
- [29] N. Foster, M.A. Clark, M.A. Jepson, B.H. Hirst, *Ulex europaeus* 1 lectin targets microspheres to mouse Peyer's patch M-cells in vivo, *Vaccine* 16 (1998) 536–541.
- [30] R. Schulte, S. Kerneis, S. Klinke, H. Bartels, S. Preger, J.P. Kraehenbuhl, E. Pringault, I.B. Autenrieth, Translocation of *Yersinia enterocolitica* across reconstituted intestinal epithelial monolayers is triggered by *Yersinia* *invasin* binding to beta1 integrins apically expressed on M-like cells, *Cell Microbiol.* 2 (2000) 173–185.
- [31] L. Belvisi, A. Bernardi, M. Colombo, L. Manzoni, D. Potenza, C. Scolastico, G. Giannini, M. Marcellini, T. Riccioni, M. Castorina, Targeting integrins: Insights into structure and activity of cyclic RGD pentapeptide mimics containing azabicycloalkane amino acids, *Bioorg. Med. Chem.* 14 (2006) 169–180.
- [32] C. Salvagnini, A. Roback, V. Pourcelle, M. Montaz, J. Marchand-Brynaert, Surface functionalization of poly(butylene terephthalate) melt blown filtration membrane by wet chemistry and photo-grafting, *J. Biomater. Sci., Polym.* (in press).
- [33] V. Pourcelle, S. Devouge, M. Garinot, V. Pr at, J. Marchand-Brynaert, PCL–PEG-based nanoparticles grafted with GRGDS peptide: surface analysis, *J. Colloid. Interface Sci.* (2007).
- [34] Y. Dong, S.S. Feng, Methoxy poly(ethylene glycol)–poly(lactide) (MPEG–PLA) nanoparticles for controlled delivery of anticancer drugs, *Biomaterials* 25 (2004) 2843–2849.
- [35] J.H. Eldridge, C.J. Hammond, J.A. Meulbroek, J.K. Staas, R.M. Gilley, T.R. Tice, Controlled vaccine release in the gut-associated lymphoid tissues. I. Orally administered biodegradable microspheres target the Peyer's patches, *J. Control. Release* 11 (1990) 205–214.
- [36] M. Shakweh, G. Ponchel, E. Fattal, Particle uptake by Peyer's patches: a pathway for drug and vaccine delivery, *Expert Opin. Drug Deliv.* 1 (2004) 141–163.
- [37] C. Prego, M. Garcia, D. Torres, M.J. Alonso, Transmucosal macromolecular drug delivery, *J. Control. Release* 101 (2005) 151–162.
- [38] D.J. Brayden, Oral vaccination in man using antigens in particles: current status, *Eur. J. Pharm. Sci.* 14 (2001) 183–189.